

Inventory of Supplemental Data

Figure S1, related to Figure 2. Quantification of side branching in outgrowths generated from decreasing dilutions of transplanted cells.

Table S1, related to Figure 2. Overview of mammary fat pad filling at decreasing dilutions of transplanted cells.

Figure S2, related to Figure 3. FACS analysis and colony formation assays. (A) Analysis of CD29 and CD24 surface markers in MECs. **(B)** Cyclin D1 is expressed in luminal but not in myoepithelial cells.

Figure S3, related to Figure 4. CD24/CD49f sorted populations. (A) Cytokeratin-14 (K14)/E-cadherin co-staining of CD24^{Med}CD49f^{Hi} - and CD24^{Hi}CD49f^{Low} - derived colonies. **(B)** CD61 expression in CD24^{Med}CD49f^{Hi} and CD24^{Hi}CD49f^{Low} populations. **(C)** The CD24^{Hi}CD49f^{Low} population contains bi-potential progenitor activity.

Figure S4, related to Figure 5. Defects in luminal epithelial differentiation. (A) Luminal differentiation defects in Cyclin D1^{KE/KE} outgrowths. **(B)** Characterization of CD24^{High} and CD24^{Low} populations.

Supplemental Data

Legends for Supplemental Figures and Table.

Figure S1, related to Figure 2. Quantification of side branching in outgrowths generated from decreasing dilutions of transplanted cells. The graph shows the number of side sprouts per mm of duct (the number of sprouts observed between a major ductal bifurcation and a terminal end bud (TEB), or between two major ductal bifurcations, were counted and the number divided by the distance in mm). Although the differences in side branching were significant between WT and KE outgrowths for all dilutions analyzed (p values < 0.0001), there was not intra-group variation between different dilutions. Error bars indicate mean \pm SD.

Table S1, related to Figure 2. Overview of mammary fat pad filling at decreasing dilutions of transplanted cells. The table shows the percentage of transplants that grew but did not fill the fat pad when 50K, 10K, or 2K cells of either genotype were transplanted (K=1,000).

Figure S2, related to Figure 3. FACS analysis and colony formation assays. (A) Analysis of CD29 and CD24 surface markers in MECs. Flow cytometry analysis for the expression of the surface markers CD29 and CD24 does not reveal a significant difference in the percentage of the CD24^{Med}CD29^{Hi} cells when cyclin D1^{KE/KE} MECs are compared to cyclin D1^{+/+} MECs. These profiles have been gated for CD45(-) cells. Error bars indicate mean \pm SD. **(B) Cyclin D1 is expressed in luminal but not in myoepithelial cells.** Immunofluorescence staining of a myoepithelial and a luminal colony for SMA (green) and cyclin D1 (red) shows that

myoepithelial cells do not stain positive for cyclin D1. However, cyclin D1 was readily detected in luminal cells from the luminal colony. Scale bar, 50 μ m.

Figure S3, related to Figure 4. CD24/CD49f sorted populations. (A) Cytokeratin-14

(K14)/E-cadherin co-staining of CD24^{Med}CD49f^{Hi} - and CD24^{Hi}CD49f^{Low} - derived colonies.

Freshly sorted CD24^{Hi}CD49f^{Low} and CD24^{Med}CD49f^{Hi} cells from either genotype were directly embedded in matrigel. After 5 days, acinar and solid colonies were subjected to

immunofluorescence for the detection of the myoepithelial marker keratin-14 (K14, green) and the luminal epithelial marker E-cadherin (red). Scale bar, 50 μ m. **(B) CD61 expression in**

CD24^{Med}CD49f^{Hi} and CD24^{Hi}CD49f^{Low} populations. Expression of CD61 in CD24^{Hi}CD49f^{Low}

and CD24^{Med}CD49f^{Hi} populations was analyzed by qRT-PCR. The CD24^{Hi}CD49f^{Low} population derived from cyclin D1^{KE/KE} mammary glands shows reduced CD61 mRNA levels compared to the same population derived from cyclin D1^{WT/WT} mammary glands (p value < 0.05). Error bars indicate mean \pm SD. **(C) The CD24^{Hi}CD49f^{Low} population contains bi-potential progenitor**

activity. CD24^{Hi}CD49f^{Low} and CD24^{Med}CD49f^{Hi} populations derived from wild-type mammary glands were transplanted in either cleared fat pads of nulliparous (virgin) mice, or cleared fat

pads of pregnant hosts. The number of successful outgrowths upon transplantation of 5 \times 10⁴ sorted cells and the percent of fat pad filling is indicated.

Figure S4, related to Figure 5. Defects in luminal epithelial differentiation. (A) Luminal

differentiation defects in Cyclin D1^{KE/KE} outgrowths. Immunofluorescence staining of ducts

from transplant outgrowths shows that cytokeratin-6 (CK6) positive cells reside in the inner layer of ducts and co-express GATA-3 but not SMA. Notice that cyclin D1^{KE/KE} ductal outgrowths do

not exhibit any detectable CK6 positive cells and also display reduced staining for GATA-3. Arrow indicates a CK6 positive cell also expressing GATA-3 as shown at higher magnification in the inset. Scale bar, 40 μ m. **(B) Characterization of CD24^{High} and CD24^{Low} populations.** Immunofluorescence staining for SMA and E-cadherin (staining done separately and both in green) of cyclin D1^{+/+} and cyclin D1^{KE/KE} MECs that were sorted for CD24 expression and cytopun directly onto slides. CD24L=CD24^{Low}; CD24H= CD24^{High}. Scale bar, 50 μ m.

Table S1

Number of Cells Transplanted						
	50K		10K		2K	
Genotype	WT	KE	WT	KE	WT	KE
% Non-filling	25 (1/4)	100 (4/4)	20 (1/5)	75 (3/4)	25 (1/4)	75 (3/4)

Table S1

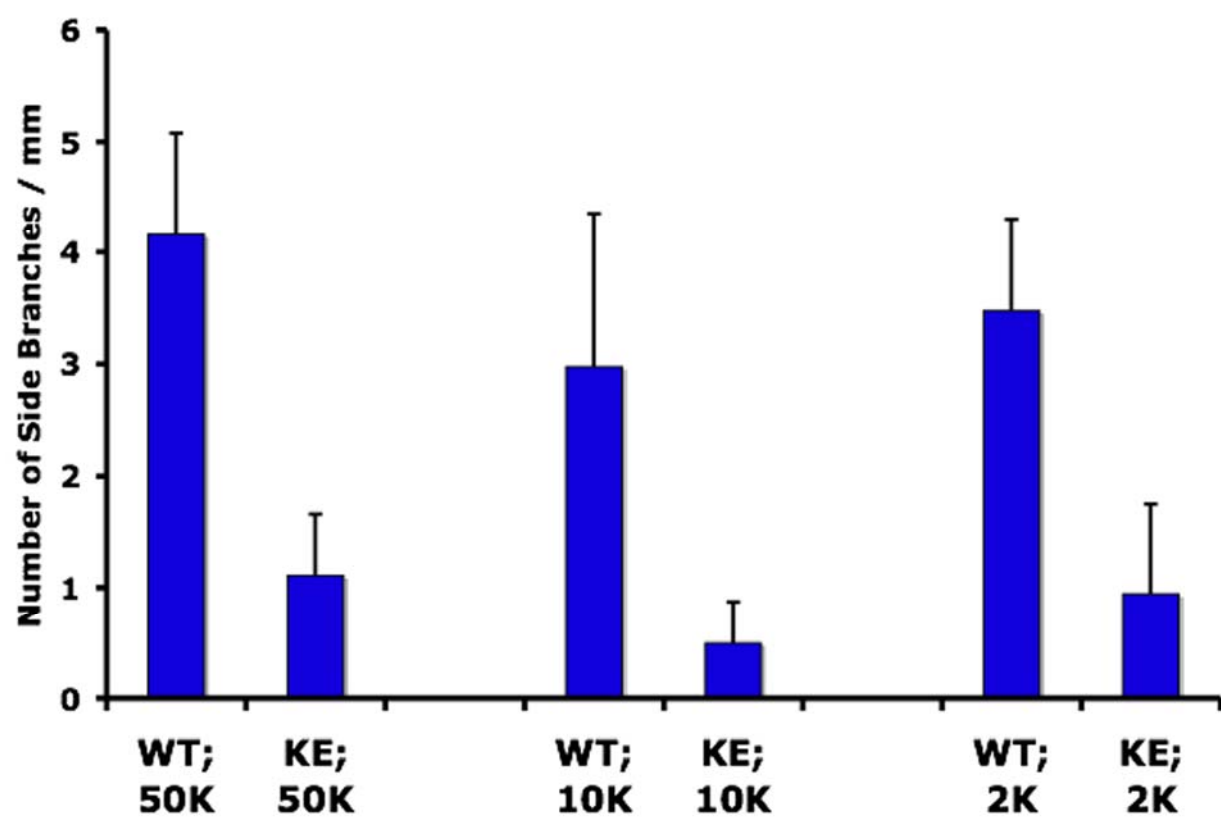
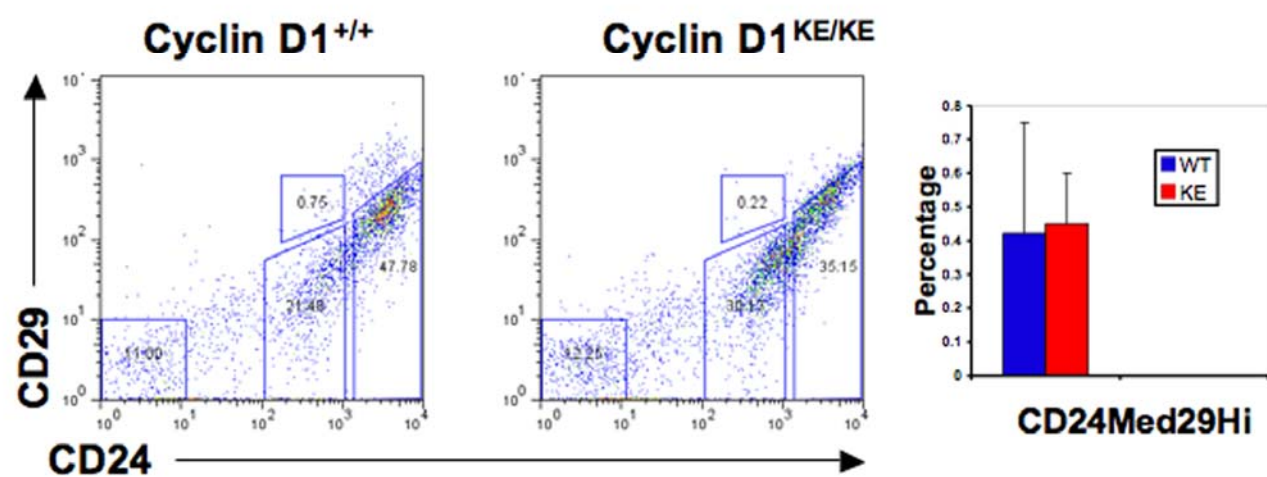
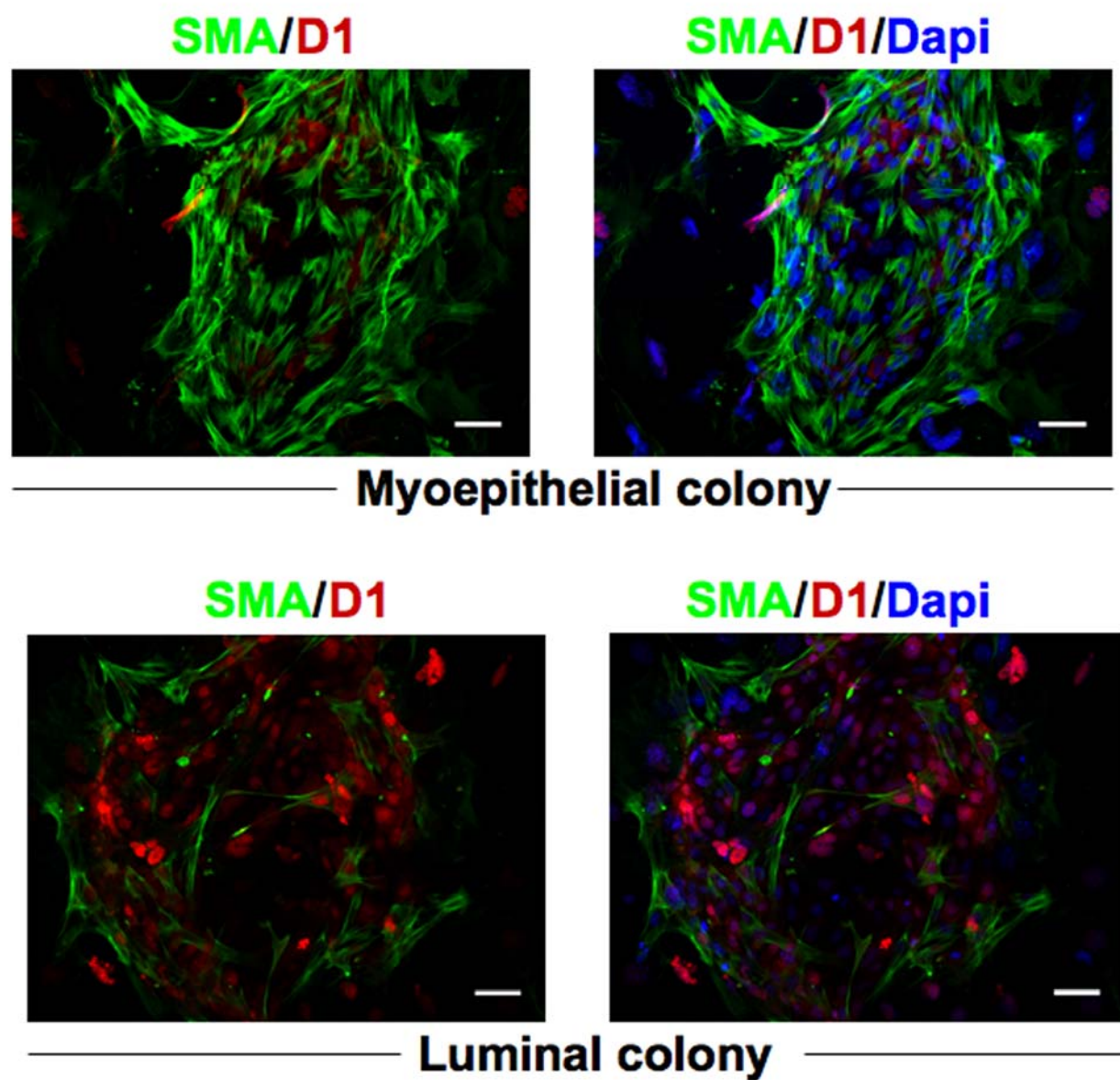


Figure S1

A**B****Figure S2**

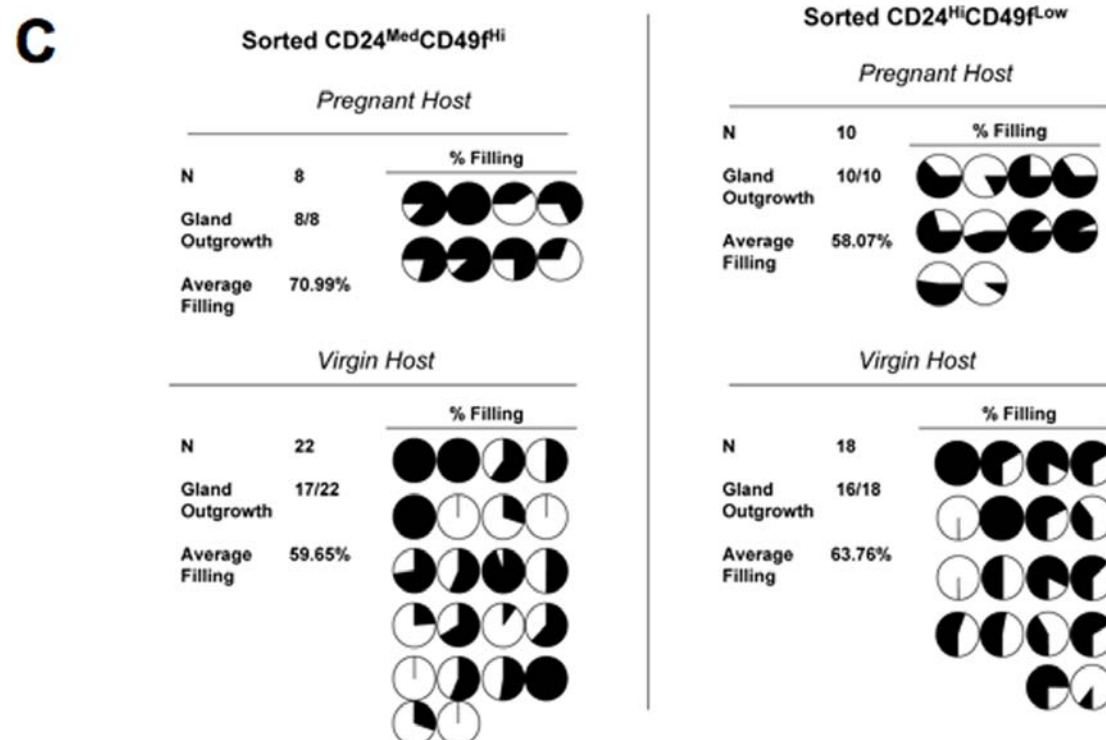
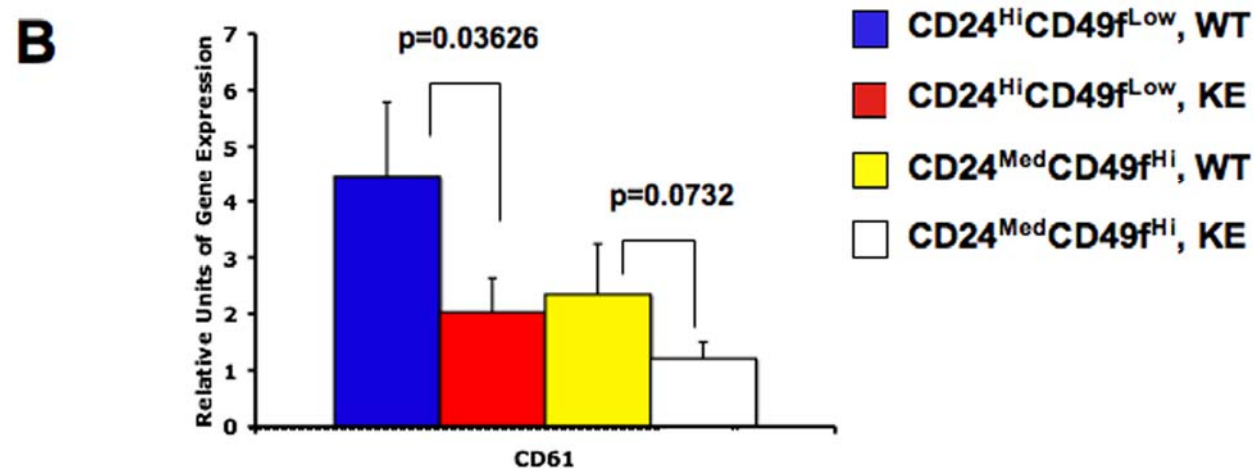
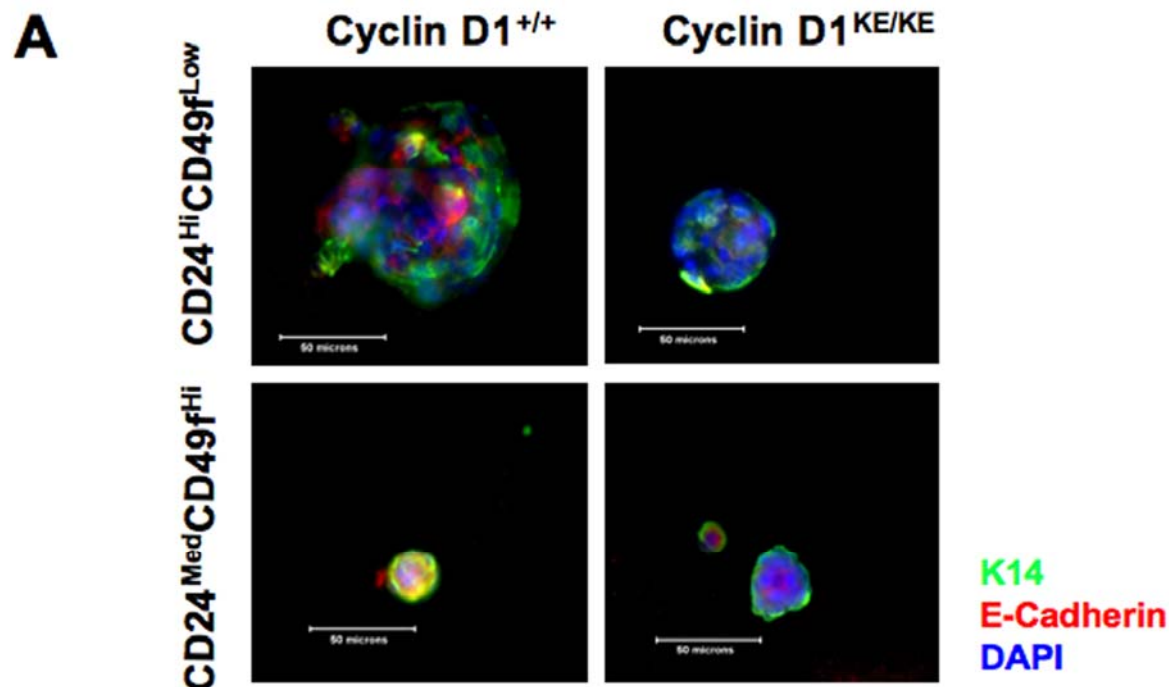


Figure S3

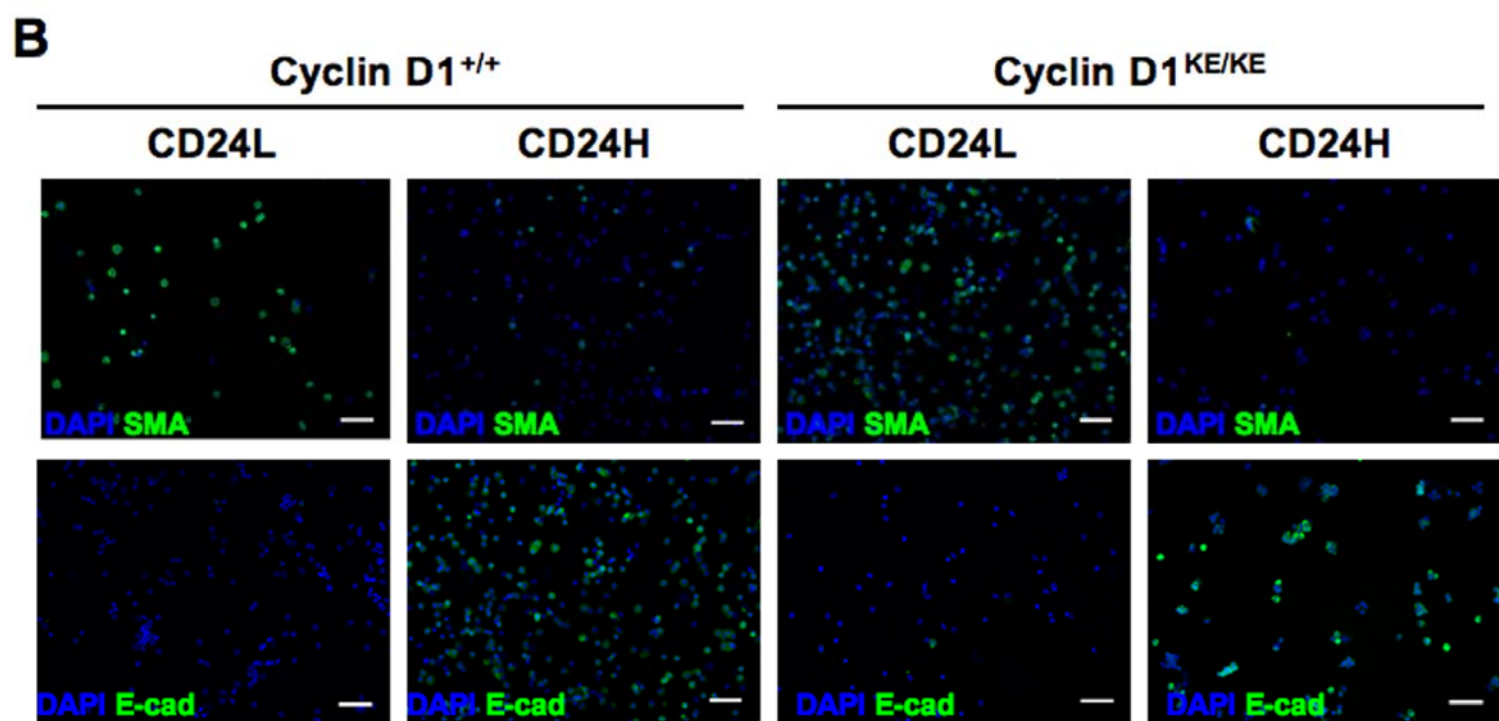
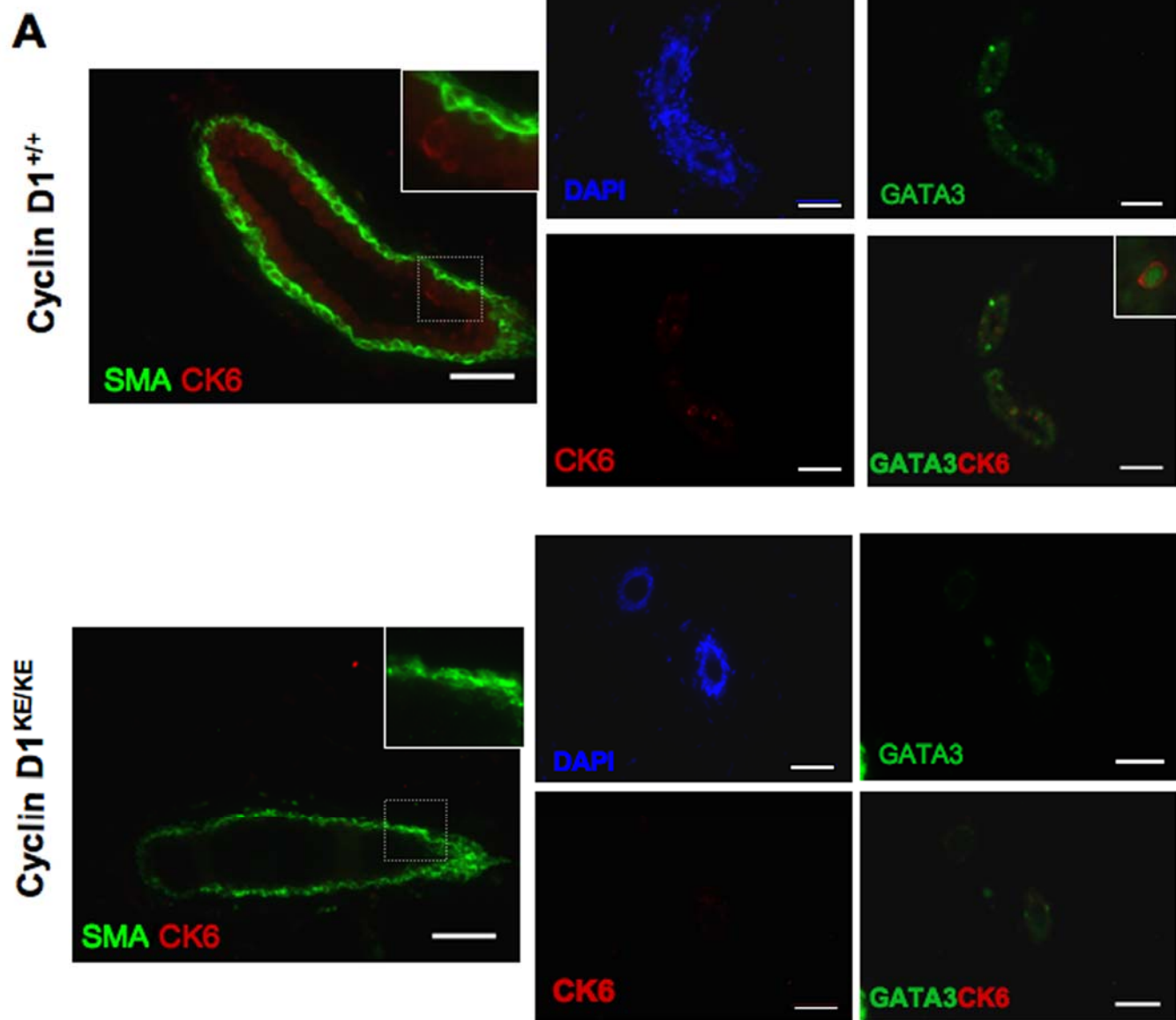


Figure S4